Nonlinearity, Scaling Trends of Quasi-Ballistic Graphene Field Effect Transistors Targeting RF Applications

Munindra (kumar.muninder90@gmail.com)
Delhi Technological University https://orcid.org/0000-0002-7305-4443
Deva Nand
Delhi Technological University

Research Article

Keywords: Graphene field effect transistor, Quasi-ballistic transport, Nonlinearity, Harmonic and intermodulation distortion.

Posted Date: May 6th, 2021

DOI: https://doi.org/10.21203/rs.3.rs-474403/v1

Nonlinearity, Scaling Trends of Quasi-Ballistic Graphene Field Effect Transistors Targeting RF Applications

Declaration

I am in full confidence conform that for this manuscript we do not any conflict of interest

Munindra, Deva Nand

Electronics and Communication Engineering, Delhi Technological University, Delhi, India

Bawana Rd, Shahbad Daulatpur Village, Rohini, Delhi, 110042

About Authors

MUNINDRA was born in Roorkee, Uttrakhand-India in August 1990. He received the B. Tech. and M. Tech. degrees in Electronic and Communication engineering from the Uttrakhand Technical University, Dehradun, in 2011 and Natiotional Institute of Technology (NIT) Delhi in 2016 respectively. Currently he is pursing the Ph.D. degree in Electronic and Communication engineering from Delhi Technological University, Delhi-India since 2017.

Nonlinearity, Scaling Trends of Quasi-Ballistic Graphene Field Effect Transistors Targeting RF Applications

Abstract— Ballistic transport based graphene field effect transistor (GFET) is the emerging nanoelectronics device technology, which is promising to add a new dimension to electronic devices and to replace conventional silicon technology, especially for radio frequency applications. In this paper, the radio (GHz) frequency static linearity and nonlinearity performance potential are analyzed for the ballistic approach GFET under the ballistic transport regime. This work explores the static linearity of graphene FET mathematically under the quasi-ballistic transport regime along with the scaling outlook of the GFETs at four different channel lengths. The proposed model explores close mathematical expressions for Harmonic distortion, intermodulation distortion, and interception points and also depicted them in graphical form. The second and third order harmonics and intermodulation distortions are analyzed with help of mathematical analysis of drain current equation formulated using Mckelvey's flux theory (MFT). The presented expressions are validated through a nonlinear output characteristic curve (Drain current versus drain voltage) at channel lengths of 140, 240, 300, and 1000 nm. The nonlinearity effect and its impact on the radio frequency electronic application of the quasi-ballistic and ballistic approach GFETs is one of the important prospects and is tabulated in Table 1 for more clarity with the particular models and respective frequencies.

Keywords: Graphene field effect transistor, Quasi-ballistic transport, Nonlinearity, Harmonic and intermodulation distortion.

Introduction:

GFETs modeling and simulation play an important role in the research and development of the Technology Computer-Aided Design (TCAD) tools which are dedicated to 2D electronic device design. Electronic device designing tools are useful to simulate and develop advanced device structure and circuit applications. Conventional FETs modeling was dedicated to silicon technology only. Since silicon technology based electronics has reached its scalable limit. Further, channel length scaling for the Si based MOSFET produces many short channel effects and thermal heat in the integrated circuits (ICs). Thus for the advancement of technology with time and hilarious research interest in the two dimensional MOSFET technology recently, graphene is found as a novel electronic material. Graphene is an atomically thick 2D material and transition metal chalcogenide (TMDs) are being researched with great effort to use their exceptional electronic properties. Graphene is the most promising and research interest 2D material for future electronic devices as it has very high electron mobility (2×10^5 $cm^2V^{-1}S^{-1}$), which can reduce many of the short channel effects at nanometer technology [1-3]. While graphene on silicon oxide base degrades its most fascinating properties (very high electron mobility ~ 10^4 $cm^2V^{-1}S^{-1}$) also no bandgap in graphene limits the scope of graphene based logic transistor. The literature [4-6] has also reported about the scope of graphene based high speed and RF electronics application. The hexagonal Boron Nitride (hBN) is an appealing and supporting 2D dielectric material which shown three to four times improved electron mobility (4×10^4 $cm^2V^{-1}S^{-1}$) as a comparison to the SiO_2 as reported in [7]. Hexagonal Boron Nitride (hBN) as 2D

dielectric material also supports to improve the RF performance metrics like high-intrinsic transit frequency and unity-power-gain frequency of GFETs. Modeling and simulation of the graphene FETs with a base as Sio2/hBN has been reported since the discovery of graphene. Graphene based FETs modeling reported the very first time was graphene field effect device in 2007[8]. Many other GFETs modelling has also reported the intrinsic transit frequency comparable to or higher than similar size CMOS nanometre technology [9-12], some other reports drain current formulation for the GFETs based on drift-diffusion equation [13-15]. A virtual source technique, basic physics based [16-18] and quasi-ballistic transport mechanism or MFT based [19-21] also has been reported. Two best fit transport approaches of an electron through the channel used for the formulation of drain current are Landauer's charge based and Mckelvey's flux based. The first approach is based on the charge carrier coherence concept given by Landauer, applicable to only low level voltage and temperature [19]. The second approach is Mckelvey flux theory based. MFT techniques are compatible with standard circuit simulators for circuit designing and they can be used to analyze the GFET Model [21-22]. At the same time, Landauer approaches discussed above are not sufficient to capture all magnificent regions of GFETs along with quasi-ballistic transport mobility of charge carriers in the atomic size graphene. The focus of the proposed work is quasi-ballistic and ballistic transport GFETs, which explores the very long mean free path (300 ±100nm) for carrier density ~10 cm^{-2} at room temperature with sigma tight bonding leads to collision free transport i.e. ballistic transport approach. The linearity of the GFET models is also an important performance metric because for RF devices and circuits a very weak signal is processed in presence of strong interference. Since only a few models are reported the linearity and nonlinearity study of the GFETs, such as Static nonlinearity [23] and RF linearity [24] of GFETs

which explains the nonlinear impact of the single layer graphene at the nanometre technology of diffusive transport approach only. Since the graphene channel is ballistic transported at nm technology, there is scope for the study of nonlinearity for the quasi-ballistic and ballistic GFETs.

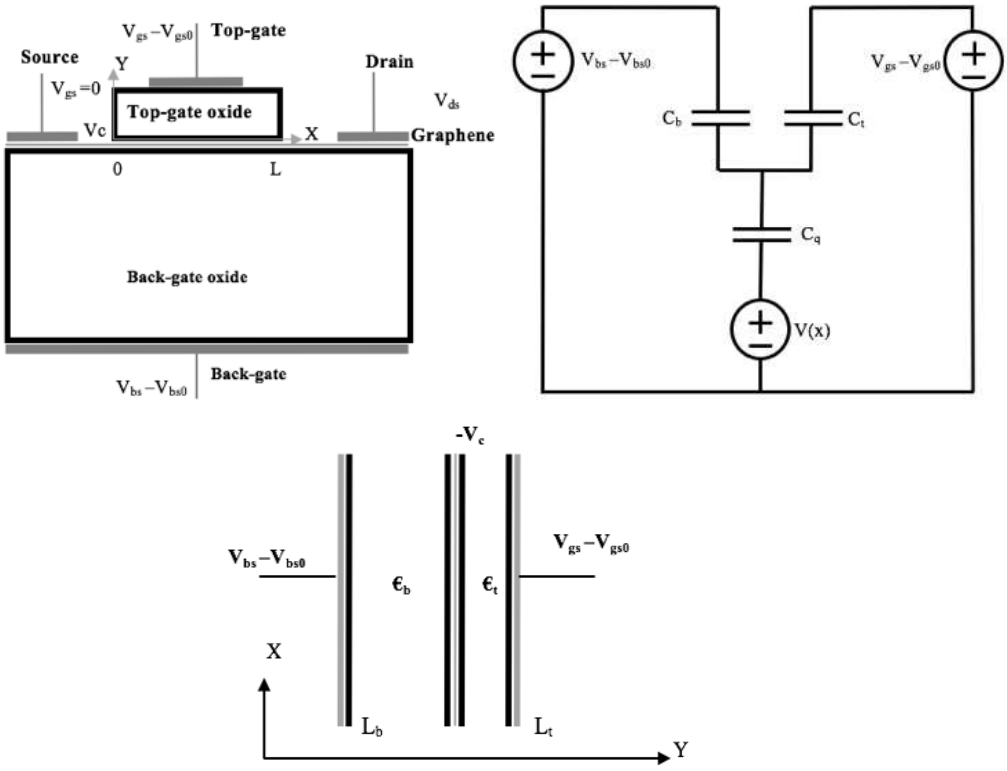

Figure 1. cross-sectional view of the proposed GFET device with the basic electrostatic parametric details, in figure 1.b equivalent capacitance of the GFET model, in figure 1.c view of the proposed model GFET with the equivalent capacitance of the GFET model of GFET.

This nonlinear study of GFETs in this work is being organized in a very explicit way, there are five sections. The first section introduces graphene properties, its limitation towards logic devices, its favorable properties towards the RF applications, and also reports hBN as a supportive dielectric bed. The section first continued to explain GFETs various modelling and lighten up the scope and research interest for the nonlinear study of quasi-ballistic GFETs, which is also a novelty of this work. Section second presents the drain current nonlinearity mathematically in detail for the quasi-ballistic approach GFET which is inspired from literature but very first time reported for

the quasi-ballistic GFETs. The proposed model applies the improved and effective mobility concept for the nonlinearity calculation. The third section validates the nonlinearity effects, discussing the proposed results and compares them with the conventional CMOS models reported earlier in literature. An appendix is also given in this work for the simplified and close study of drain current under a quasi-ballistic regime.

Static nonlinearity model:

The static nonlinearity of GFETs under quasi-ballistic regime can be calculated be expanding drain current as Taylor series

$$I_{DS} = x_1 V_{GS} + x_2 V_{GS}^2 + x_3 V_{GS}^3 + \cdots + x_n V_{GS}^n \quad (1)$$

while drain current [20] formulation based on Mckelvey's flux theory (MFT)

$$I_{DS} = \frac{Wn(x)V_{Th}(1-r_{bs})[1-\pounds_1(\omega_F-\omega_{DS})/\pounds_1(\omega_F)]}{(1+r_{bs}(1-r_{bs})\pounds_1(\omega_F-\omega_{DS})/\pounds_1(\omega_F)]} \quad (2)$$

W is here width of GFET, n(x) is charge carrier concentration in graphene channel as an ensemble of field dependent charge carrier density, n_E and field independent charge carrier density called as residual carrier density. So the total carrier concentration contributing to the calculation of drain current can be represent mathematically [22] as $n(x) = n_{EF} + n_{Res}$where field dependent density of carrier is of more important at large value of V_{CH} than (q $V_{CH} \gg K_B T$) can be written mathematically [21].

$$n_{EF} = \frac{q\pi(K_B T)^2}{(\hbar v f)^2} + \frac{(q)^3 V_{CH}|V_{CH}|}{\pi(\hbar v f)^2} \quad (3)$$

with the usual meaning of symbols, field independent charge carrier is also an ensemble of thermally excited (n_i) and electron hole puddles adding carriers [29].

$$n_{pud} = \frac{2}{\pi(\hbar v f)^2}(\Delta^2/2 + \pi^2(K_B T)^2/6) \quad (4)$$

and 2D degenerated thermal velocity V_{Th} of graphene layers is found independent of V_{GS} (gate to source voltage), which can be arranged in equations [28] $V_{Th-2D} = V_{Th}\sqrt{\pi}/2$ after putting 2 for (2D) graphene sheet. Now the next element of drain current is backscattering coefficient r_{bs}, is another parameter independent of V_{GS} directly, and can be solve mathematically as [22, 25]

$$r_{bs} = \frac{\left(\frac{1.5\,V_{ds}\mu_{eff}}{2LK_BT\lambda}\right)}{\frac{q|E|}{2K_BT}\left(1+\coth\left(\frac{Lq|E|}{2K_BT}\right)\right)+\lambda^{-1}} \tag{5}$$

with λ as mean free path in the graphene channel which can be formulated mathematically as $\lambda = \hbar\mu(\sqrt{\pi n}/2)$. Where symbols have there usual meaning. μ_{eff} is the quasi-ballistic phenomenal effective mobility given by Mathiessen's rule [27], which could be described mathematically as

$$\frac{1}{\mu_{eff}} = \frac{1}{\mu_0} + \frac{1}{\mu_B} \tag{6}$$

where μ_0 is $16\epsilon_g(\hbar vf)^2/q^3 n_{imp}$ formulated in [30] i. e. this part of mobility is inversely proportional to the injected impurity and has important role of scattering. Now the ballistic transport contributing mobility μ_B is $q\,L\,/m * V_{Th-2D}$ i. e. ballistic phenomenal mobility is inversely proportional to the thermal velocity. So as it is very obvious that total or effective mobility is depends on both factor impurity as well as very thermal velocity into the two dimensional material graphene and is independent of the gate to source voltageV_{GS}. One more parameter in drain current is$£_1(\omega_F - \omega_{DS})/£_1(\omega_F)$, is the Fermi-Dirac integral of order one defined by Blakemore. Where ω_F is equal to $(E_F - E_C)/K_BT$ and ω_{DS} is equal to$(qV_{DS})/K_BT$withE_F is equal to qV_{CH}. So first ω_F Fermi-Dirac integral is also depends upon the gate to source voltage V_{GS}. The additional and interesting fact is that V_{CH} is one more parameter depends on V_{GS}in the drain current formulation [12], which could be elaborate mathematically as function of parametric capacitances in channel of 2D GFET.

$$I_{DS} = \frac{A\left(B+CV_{CH}^{2}(x)\right)(1-r_{bs})[1-\pounds_1(\omega_F-\omega_{DS})/\pounds_1(\omega_F)]}{(1+r_{bs}+(1-r_{bs})\pounds_1(\omega_F-\omega_{DS})/\pounds_1(\omega_F)]} \quad (8)$$

where A, B and C are constant of value $W.V_{Th}$, $q\pi(K_BT)^2/3(\hbar v_F)^2$ and $q^3/\pi(\hbar v_F)^2$ are respectively, when all elementary constant has their usual meaning. Note that here in (7) the carrier density n(x) parameter includes Electric field dependent and independent but for the further calculation only n_{EF} part is used and residual carrier density to minimize the leakage current. By simplified and modified the drain current (8) in appendix and using (7) a direct relation between the gate voltages and reference voltages can be modelled as

$$I_{DS} = \frac{AB+AC\left(\frac{1}{\mathrm{C_{tox}}+\mathrm{C_{box}}+0.5\,\mathrm{C_q}}(V_{gs_{top}}-\frac{\dot{V}(x)}{2})C_{tox}-(V_{gs_{back}}-\frac{V(x)}{2})C_{box}\right)^{2}P[R]}{[(1+P-Q)(R)]} \quad (9)$$

where P, Q and R are fitting parameters, $\frac{1.5\,V_{ds}\mu_{eff}}{2L\,K_BT\lambda}$, $\frac{1.5\,V_{ds}\mu_{eff}}{(2L\,K_BT\lambda)^2}$and $exp-\frac{V_{ds}}{\mathrm{K}_B T}$, respectively function of drain voltage, effective mobility, mean free path and Channel length as mention in appendix with details.

Linearity and nonlinearity of GFET under ballistic transportation phenomenon, as state above in (1) can be calculated by differentiating the drain current (I_{DS}) with respect to gate to source voltage (V_{GS}). Thus to find coefficient of Taylor series to elaborate the nonlinearity of GFET as reported by S. Rodriguez in [23] can be done in this way $\left(V_{gs}-V_{gs0}-V_{ds}\right)$. The unknown coefficients of the Taylor's series can be find by simply differentiating the drain current equation of the Bilayer GFET. Taylor's series ($\mathrm{X_1}, \mathrm{X_2}, \mathrm{X_3}$) coefficients can be used further to formulate the harmonic distortion (HD) and intermodulation Distortions as follows

$$x_1 = \frac{\delta I_{DS}}{\delta V_{GS}}\Big| = \frac{AC(2V_{gs_{top}}*C_{tox}^2+2V_{bs_{back}}*C_{box}^2-2V_{gs_{top}}*C_{tox}*2V_{bs_{back}}*C_{tox})P[R]}{\mathrm{C_{tox}}+\mathrm{C_{box}}+0.5\,\mathrm{C_q}[(1+P-Q)(R)]} \quad (10)$$

$$x_2 = \frac{\delta 2 I_{DS}}{\delta V 3_{GS}}\Big| = -\frac{AC(2C_{tox}^2+2C_{box}^2-2V_{gs_{top}}*C_{tox}*2V_{bs_{back}}*C_{box})P[R]}{\mathrm{C_{tox}} + \mathrm{C_{box}} + 0.5\,\mathrm{C_q}[(1+P-Q)(R)]}$$

(11)

$$x_3 = \frac{\delta 3 I_{DS}}{\delta V 3_{GS}}\Big| = \frac{AC(2*2C_{tox}*C_{box})P[R]}{\mathrm{C_{tox}} + \mathrm{C_{box}} + 0.5\,\mathrm{C_q}[(1+P-Q)(R)]} \quad (12)$$

these coefficients can be use for the further calculation regards finding the nonlinearity for the quasi-ballistic transport approached GFET, which can represent mathematically as harmonic distortion and intermodulation of order first, second and third like as follows. Since to the order one is basic and useful information of device model so harmonic distortion of second order is

$$\mathrm{HD_2} = \frac{1}{2}\left|\frac{x_2}{x_1}\right| V_{GS} = \frac{(2C_{tox}^2+2C_{box}^2-2V_{gs_{top}}*C_{tox}*2V_{bs_{back}}*C_{box})V_m}{(2V_{gs_{top}}*C_{tox}^2+2V_{bs_{back}}*C_{box}^2-2V_{gs_{top}}*C_{tox}*2V_{bs_{back}}*C_{tox})} \quad (13)$$

and the harmonic distortion of third order is

$$\mathrm{HD_3} = \frac{1}{4}\left|\frac{x_3}{x_1}\right| V_{GS}^2 = \frac{(C_{tox}*C_{box})V_m^2}{(2V_{gs_{top}}*C_{tox}^2+2V_{bs_{back}}*C_{box}^2-2V_{gs_{top}}*C_{tox}*2V_{bs_{back}}*C_{tox})} \quad (14)$$

Similarly, to find the intermodulation distortion of order one is very simple and so intermodulation distortion of order second is

$$\mathrm{IM_2} = \left|\frac{x_2}{x_1}\right| V_{GS} = \frac{(2C_{tox}^2+2C_{box}^2-2V_{gs_{top}}*C_{tox}*2V_{bs_{back}}*C_{box})V_m}{(2V_{gs_{top}}*C_{tox}^2+2V_{bs_{back}}*C_{box}^2-2V_{gs_{top}}*C_{tox}*2V_{bs_{back}}*C_{tox})} \quad (15)$$

And the intermodulation distortion of third order

$$\mathrm{IM_3} = \frac{3}{4}\left|\frac{x_3}{x_1}\right| V_{GS}^2 = \frac{3(C_{tox}*C_{box})V_m^2}{4(2V_{gs_{top}}*C_{tox}^2+2V_{bs_{back}}*C_{box}^2-2V_{gs_{top}}*C_{tox}*2V_{bs_{back}}*C_{tox})} \quad (16)$$

Result and discussion:

The nonlinear study of the quasi-ballisticm GFETs can be done statically as well as by the observation of potential performance at high frequency. The high frequency performance of GFETs gets affected due to the presence of the parasitic capacitances at short channel length that adds nonlinearity effect to the GFETs characteristic. The

above section explains static nonlinearity in mathematical equations and this section present and validates the graphical and tabular form of the nonlinearity of the GFETs under the quasi-ballistic regime in a very novel way. Nonlinearity effects and influences the GFETs performance by the addition of harmonic and intermodulation distortions, which results in lowering the gain of the GFETs, shifts in the DC offsets, and cross modulation of the AM/PM, etc.

Table 1 listed the nonlinearity characteristics of high frequency operation of GFETs.

Ref.	**Operating Frequency**	**IIP3 (dBm)**	**Conversion loss (dB)**	**L(um)**
[31]	10MHz	13.8	~30 to 40	2
[32]	30GHz	12.8	19	0.5
[33]	NA	4.9	20-22	1
[34]	NA	22	~15	0.25
[34]	NA	27	10	2
[35]	2GHz	19	5	0.75
[36]	4.3GHz	30	10	0.24
[37]	300MHz	20	15	0.5
[38]	NA	17	17	2.4
[24]	NA	13.8	22	0.44
proposed	30GHz	12.6	18.4	0.14
proposed	30GHz	12.8	18.8	0.30

The Table 1 present and compare the RF nonlinearity characteristic of the GFETs at different channel length and frequency. Table 1 also presents IIP3 (input intercept points) of the third order and total gain compression for the available and proposed model. The bar graph given in Fig. 2 shows the static and RF nonlinearity by the column, stacked, and area chart for the proposed modelled, and CMOS field effect devices. The analytical outcomes of the proposed GFET model and simulated result values are compared with the CMOS technology with help of harmonic distortions and intermodulation distortions of second order and third order. HDs and IMs are validating the nonlinear character of the proposed ballistic GFET model.

This section validates and compares the dynamic nonlinear characteristic curves of ballistic transport nature GFET at various channel lengths (L = 140, 240, 300, and 1000 nm) as shown in below figure 3. Nonlinearity effects can be very easily visualized in figure 3.a, 3.b, 3.c, and 3.d, at very low gate voltage I-V characteristic curve show nonlinear gradual increment and turn with kinks at a higher value of drain voltage. Characteristic curve crossover for the different gate voltages can be easily seen in figure 3. which is because of these kinks in the I-V characteristic curves. These crossovers in characteristic curves for the increasing gate voltage prove and justify the linearity, scaling and nonlinearity of the characteristic behavior of drain current of the ballistic approached GFETs. The scaling of channel length and nonlinearity of drain current is very much related as seen in all four graphs of figure 3 at various channel length of (L = 140, 240, 300, and 1000 nm) for increasing drain to source voltage (from 0 to 2 V). The figure 3.a drain current versus drain voltage output characteristic curve is showing the highly nonlinear behaviour of the curve at 1000nm. The figure 3.b at 300nm also shows nonlinearity at low (0 to 1V) drain voltage and shows linear shape after 1V drain voltage value. The figure 3.c shows the almost linear curve of current and voltage, while a kink is present at 1.25V at a low gate voltage value and this kink is absent at a higher value of gate voltage. The figure 3.d is shown the linear curve of output drain current and voltage at all (0 to 2V) drain voltage. This work inspired by the static nonlinearity of the non-ballistic transport approach [23], presents the static and dynamic nonlinearity of the quasi-ballistic GFETs model. The validation and comparison have been done with help of bar graphs (figure 2), RF frequency nonlinearity table 1, and dynamic nonlinearity drains current characteristic (figure 3). The dynamic nonlinear characteristic behaviour very well matched and compared with the reported work [16,

21]. All the simulated results are shown in Fig. 3 are drawn by lines while all the analytical outcome values are drawn by squares (symbols).

Figure 2: Non-linear behaviour of the bilayer graphene field effect transistors (GFET) shown with bar graph as the static nonlinearity by the column, stacked and area chart for the proposed modelled, and CMOS field effect devices.

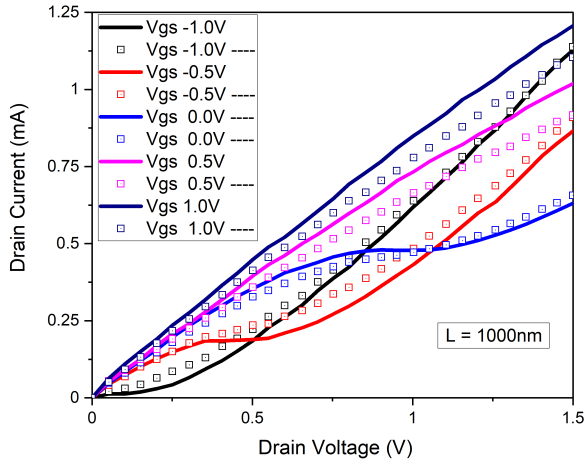

a

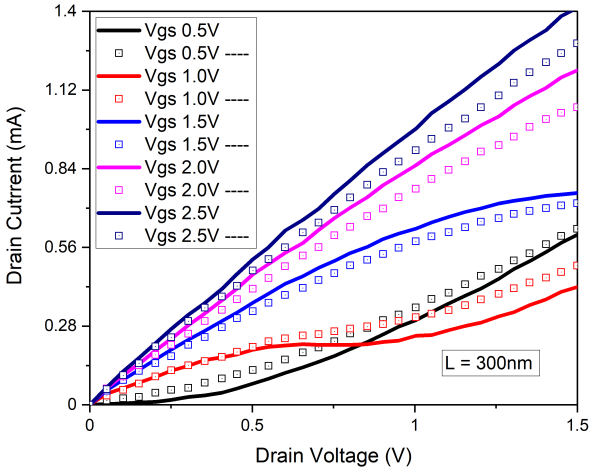

b

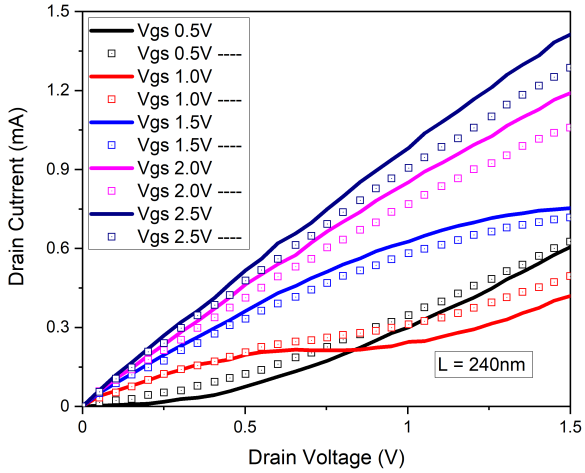

c

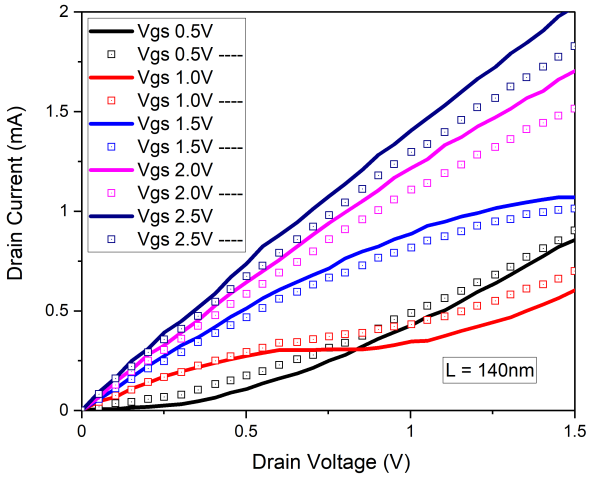

d

Figure 3: Non-linear characteristic behavior of the quasi-ballistic GFETs. figure 3.a I_{ds} vs V_{ds} output characteristic curve is showing highly nonlinear behavior of curve at 1000nm. Figure. 3.b at 300nm also shows nonlinearity at low (0 to 1V) drain voltage and shows linear shape after 1V drain voltage value. Figure 3.c shows the almost linear curve of current and voltage at 240nm, while a kink is present at 1.25V at a low gate voltage value. Figure 3.d is shown the linear curve of output drain current and voltage at all (0 to 2V) drain voltage at 140nm. All the simulated results are shown in figure 3 are drawn by lines while all the analytical outcome values are drawn by squares (symbols).

Conclusion:

Since the nonlinearity of the particular devices is a great source of noise in the nanoelectronics device application based on GFETs. So the linearity and nonlinearity of the ballistic transport approach GFETs is of paramount necessity. Thus an explicit nonlinearity characteristic behaviour of the ballistic transport approach GFET presented in this work has a significant importance in this advanced nanotech era. This work is a comparison of GFETs at various scaling channel lengths for the proposed model and

simulation results in line graphs.

Decleration of Interest:

There for this work we donot have any conflict of interest.

Apendix:

The drain current for the four terminal GFET devices can be modified for simplicity of the calculation and to make modelling effective to the EDA tool developers. From (3) and (4) total charge density can be compiled as

$$n(x) = \frac{(q)^3 V_{CH}|V_{CH}|}{\pi(\hbar v_f)^2} + C \ldots\ldots \quad (17)$$

where *C* here is constant with the useful scientific values of the symbols used in (3) and (4) and $\boldsymbol{v_f}$ Fermi velocity is 10^6 m/sec at room temperature[1]. For the particular value of extrinsic electric field (E), fixed channel length (140nm, 300nm) and mean free path length, mentioned in detail in the introduction section backscattering coefficient (r_{bs}) could also be simplified in an explicit math equation from (5) as a function of V_{ds} and $\mu_{\boldsymbol{eff}}$, where *C* is again constant with other notations as usual scientific symbols

$$r_{bs} = \left(\frac{1.5\, V_{ds}\mu_{eff}}{2L\, K_B T\lambda}\right)/C \quad (18)$$

and Fermi-Dirac integral solved by Blackmore [39, 26] of order one can also be simplified more explicitly as a function of V_{ds} only as

$$\mathfrak{L}_1(\omega_F) = \int_0^{\infty}\left[\frac{1}{1+exp\frac{(E-E_F)}{K_B T}}\right]dE \quad (19)$$

and which can be approximated as $exp - \frac{(E-E_F)}{K_B T}$ and so $\mathfrak{L}_{\boldsymbol{1}}(\omega_{\boldsymbol{F}} - \omega_{\boldsymbol{DS}})/\mathfrak{L}_{\boldsymbol{1}}(\omega_{\boldsymbol{F}})$ can be a function of drain voltage only as $exp - \frac{V_{ds}}{K_B T}$ after simplification of the exponential

math's. Thus a proper drain current and gate voltage relation can be present mathematically as

$$I_{DS} = \frac{A\left(B+CV_{CH}^{2}(x)\right)\left(1-\frac{1.5\,V_{ds}\mu_{eff}}{2L\,K_B T\lambda}\right)[1-e^{-\mathrm{Vds/kBT}}]}{[(1+\frac{1.5\,V_{ds}\mu_{eff}}{2L\,K_B T\lambda}-\left(\frac{1.5\,V_{ds}\mu_{eff}}{2L\,K_B T\lambda}\right)^{2})(e^{-\mathrm{Vds/kBT}})]} \quad (20)$$

References:

[1] NovoselovKostya S., Andre K. Geim, Sergei V. Morozov, D. Jiang, Y_ Zhang, Sergey V. Dubonos, Irina V. Grigorieva, and Alexandr A. Firsov. "Electric field effect in atomically thin carbon films." *Science*306, no. 5696: 666-669, Oct (2004).

[2] Geim, A. K., and K. S. Novoselov. "The rise of graphene" Nature materials, 6: 183–191, *March* (2007).

[3] Schwierz, Frank. "Graphene transistors: status, prospects, and problems." *Proceedings of the IEEE* 101, no. 7: 1567-1584, May (2013).

[4] Geim Andre Konstantin, "Graphene: status and prospects." *Science*324, no. 5934: 1530-1534, Jun (2009).

[5] Novoselov, Konstantin S., V. I. Falko, L. Colombo, P. R. Gellert, M. G. Schwab, and K. Kim. "A roadmap for graphene." *Nature*490, no. 7419: 192-200, Oct (2012).

[6] Chen, Jian-Hao, Chaun Jang, Shudong Xiao, Masa Ishigami, and Michael S. Fuhrer. "Intrinsic and extrinsic performance limits of graphene devices on SiO_2," *Nature nanotechnology*3, no. 4: 206-209, Apr (2008).

[7] Dean, Cory R., Andrea F. Young, InancMeric, Chris Lee, Lei Wang, Sebastian Sorgenfrei, Kenji Watanabe et al. "Boron nitride substrates for high-quality graphene electronics." *Nature nanotechnology*5, no. 10: 722-726, Oct (2010).

[8] Lemme, Max C., Tim J. Echtermeyer, Matthias Baus, and Heinrich Kurz. "A graphene field-effect device." *IEEE Electron Device Letters*28, no. 4: 282-284, Mar (2007).

[9] Han, Shu-Jen, Keith A. Jenkins, Alberto Valdes Garcia, Aaron D. Franklin, Ageeth A. Bol, and WilfriedHaensch. "High-frequency graphene voltage amplifier." *Nano letters*11, no. 9: 3690-3693, Sep (2011).

[10] Lin, Yu-Ming, Damon B. Farmer, Keith A. Jenkins, Yanqing Wu, Joseph L. Tedesco, Rachael L. Myers-Ward, Charles R. Myers-Ward, D. Kurt Gaskill, Christos Dimitrakopoulos, and PhaedonAvouris. "Enhanced performance in epitaxial graphene FETs with optimized channel morphology." *IEEE Electron Device Letters*32, no. 10: 1343-1345, Sep (2011).

[11] Liao, Lei, Yung-Chen Lin, MingqiangBao, Rui Cheng, Jingwei Bai, Yuan Liu, Yongquan Qu, Kang L. Wang, Yu Huang, and XiangfengDuan. "High-speed graphene transistors with a self-aligned nanowire gate." *Nature* 467, no. 7313: 305-308, Sep (2010).

[12] Rodriguez, Saul, Sam Vaziri, Anderson Smith, Sebastien Fregonese, Mikael Ostling, Max C. Lemme, and Ana Rusu. "A comprehensive graphene FET model for circuit design." *IEEE Transactions on Electron Devices*61, no. 4: 1199-1206, Feb (2014).

[13] Zebrev, Gennady I., Alexander A. Tselykovskiy, Daria K. Batmanova, and Evgeny V. Melnik. "Small-signal capacitance and current parameter modeling in

large-scale high-frequency graphene field-effect transistors." *IEEE transactions on electron devices*60, no. 6: 1799-1806, May (2013).

[14] Pasadas, Francisco, and David Jiménez. "Large-signal model of graphene field-effect transistors—Part I: Compact modeling of GFET intrinsic capacitances." *IEEE Transactions on Electron Devices*63, no. 7: 2936-2941, May (2016).

[15] Pasadas, Francisco, and David Jiménez. "Large-signal model of graphene field-effect transistors—Part II: Circuit performance benchmarking." *IEEE Transactions on Electron Devices*63, no. 7: 2942-2947, May (2016).

[16] Jimenez, David, and Oana Moldovan. "Explicit drain-current model of graphene field-effect transistors targeting analog and radio-frequency applications." *IEEE Transactions on Electron Devices*58, no. 11: 4049-4052, Sep (2011).

[17] Jiménez, David. "Explicit drain current, charge and capacitance model of graphene field-effect transistors." *IEEE transactions on electron devices*58, no. 12: 4377-4383, Oct (2011).

[18] Aguirre-Morales, Jorge-Daniel, Sebastien Fregonese, Chhandak Mukherjee, CristellManeux, and Thomas Zimmer. "An accurate physics-based compact model for dual-gate bilayer graphene FETs." *IEEE Transactions on Electron Devices*62, no. 12 Oct (2015): 4333-4339.

[19] Ganapathi, Kartik, Youngki Yoon, Mark Lundstrom, and SayeefSalahuddin. "Ballistic IV characteristics of short-channel graphene field-effect transistors: Analysis and optimization for analog and RF applications." *IEEE transactions on electron devices* 60, no. 3: 958-964, Feb (2013).

[20] Hu, Guangxi, Shuyan Hu, Ran Liu, Lingli Wang, Xing Zhou, and Ting-Ao Tang. "Quasi-ballistic transport model for graphene field-effect transistor." *IEEE transactions on electron devices*60, no. 7: 2410-2414, Jun (2013).

[21] Upadhyay, Abhishek Kumar, Ajay Kumar Kushwaha, and Santosh Kumar Vishvakarma. "A unified scalable quasi-ballistic transport model of GFET for circuit simulations." *IEEE Transactions on Electron Devices* 65, no. 2: 739-746, Dec (2017).

[22] Upadhyay, Abhishek Kumar, Ajay Kumar Kushwaha, PriyankRastogi, Yogesh Singh Chauhan, and Santosh Kumar Vishvakarma. "Explicit Model of Channel Charge, Backscattering, and Mobility for Graphene FET in Quasi-Ballistic Regime." *IEEE Transactions on Electron Devices* 65, no. 12 :5468-5474, Nov (2018).

[23] Rodriguez, Saul, Anderson Smith, Sam Vaziri, Mikael Ostling, Max C. Lemme, and Ana Rusu. "Static nonlinearity in graphene field effect transistors." *IEEE Transactions on Electron Devices* 61, no. 8: 3001-3003, Jun (2014).

[24] Alam, Ahsan Ul, Kyle David Holland, Michael Wong, Sabbir Ahmed, Diego Kienle, and Mani Vaidyanathan. "RF linearity performance potential of short-channel graphene field-effect transistors." *IEEE Transactions on Microwave Theory and Techniques* 63, no. 12: 3874-3887, Nov (2015).

[25] Rahman, Anisur, and Mark S. Lundstrom. "A compact scattering model for the nanoscale double-gate MOSFET."*IEEE Transactions on Electron Devices* 49, no. 3: 481-489, Aug (2002).

[26] McKelvey, J. P., and J. C. Balogh. "Flux methods for the analysis of transport problems in semiconductors in the presence of electric fields." *Physical Review* 137, no. 5A: A1555, Mar (1965).

[27] Shur, Michael S. "Low ballistic mobility in submicron HEMTs." *IEEE Electron Device Letters* 23, no. 9: 511-513, Nov (2002).

[28] Saad, Ismail, Michael LP Tan, Hui Hii, Razali Ismail, and Vijay K. Arora. "Ballistic mobility and saturation velocity in low-dimensional nanostructures." *Microelectronics Journal* 40, no. 3: 540-542, Mar (2009).

[29] Tian, Jing, AnestisKatsounaros, Darryl Smith, and Yang Hao. "Graphene field-effect transistor model with improved carrier mobility analysis." *IEEE Transactions on Electron Devices* 62, no. 10: 3433-3440, Aug (2015).

[30] Champlain, James G. "A first principles theoretical examination of graphene-based field effect transistors." *Journal of Applied Physics* 109, no. 8 Apr (2011): 084515.

[31] Wang, Han, Allen Hsu, Justin Wu, Jing Kong, and Tomas Palacios. "Graphene-based ambipolar RF mixers." *IEEE Electron Device Letters* 31, no. 9: 906-908, Jul (2010).

[32] Habibpour, Omid, Josip Vukusic, and Jan Stake. "A 30-GHz integrated subharmonic mixer based on a multichannel graphene FET." *IEEE Transactions on Microwave Theory and Techniques* 61, no. 2: 841-847, Jan (2013).

[33] Andersson, Michael A., OmidHabibpour, Josip Vukusic, and Jan Stake. "Resistive graphene FET subharmonic mixers: Noise and linearity assessment." *IEEE transactions on microwave theory and techniques* 60, no. 12 Oct (2012): 4035-4042.

[34] Moon, J. S., H-C. Seo, M. Antcliffe, D. Le, C. McGuire, A. Schmitz, L. O. Nyakiti et al. "Graphene FETs for zero-bias linear resistive FET mixers." *IEEE Electron Device Letters* 34, no. 3: 465-467, Feb (2013).

[35] Madan, H., M. J. Hollander, M. LaBella, R. Cavalero, D. Snyder, Joshua Alexander Robinson, and S. Datta. "Record high conversion gain ambipolar graphene mixer at 10GHz using scaled gate oxide." In *2012 International Electron Devices Meeting*, pp. 4-3. IEEE, Dec (2012).

[36] Madan, Himanshu, Matthew J. Hollander, Joshua A. Robinson, and SumanDatta. "Analysis and benchmarking of graphene based RF low noise amplifiers." In *71st Device Research Conference*, pp. 41-42. IEEE, Jun (2013).

[37] Jenkins, K. A., D. B. Farmer, S-J. Han, C. Dimitrakopoulos, S. Oida, and A. Valdes-Garcia. "Linearity of graphene field-effect transistors." *Applied Physics Letters* 103, no. 17: 173115, Oct (2013).

[38] Parrish, Kristen N., and DejiAkinwande. "Impact of contact resistance on the transconductance and linearity of graphene transistors." *Applied Physics Letters* 98, no. 18: 183505, May (2011).

[39] Blakemore, John Sydney. *Semiconductor statistics*. Courier Corporation, (2002).

Table 1: listed the nonlinearity characteristics of high frequency operation of GFETs.

Figure 1: cross-sectional view of the proposed GFET device with the basic electrostatic parametric details, in figure 1.b equivalent capacitance of the GFET model, in figure 1.c view of the proposed model GFET with the equivalent capacitance of the GFET model of GFET.

Figure 2: Non-linear behaviour of the bilayer graphene field effect transistors (GFET) shown with bar graph as the static nonlinearity by the column, stacked and area chart for the proposed modelled, and CMOS field effect devices.

Figure 3: Non-linear characteristic behavior of the quasi-ballistic GFETs. figure 3.a I_{ds} vs V_{ds} output characteristic curve is showing highly nonlinear behavior of curve at 1000nm. Figure. 3.b at 300nm also shows nonlinearity at low (0 to 1V) drain voltage and shows linear shape after 1V drain voltage value. Figure 3.c shows the almost linear curve of current and voltage at 240nm, while a kink is present at 1.25V at a low gate voltage value. Figure 3.d is shown the linear curve of output drain current and voltage at all (0 to 2V) drain voltage at 140nm. All the simulated results are shown in figure 3 are drawn by lines while all the analytical outcome values are drawn by squares (symbols).

Figures

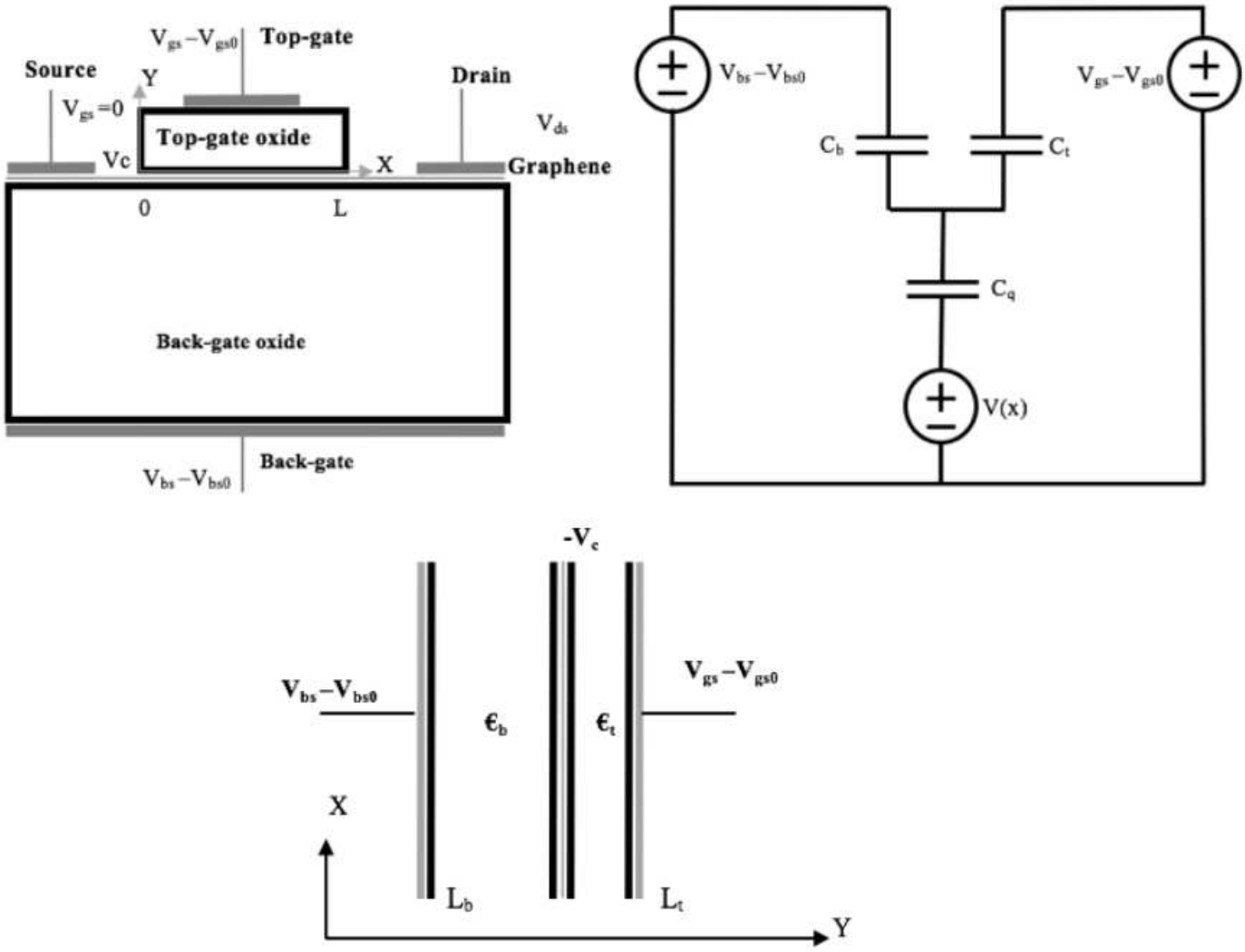

Figure 1

cross-sectional view of the proposed GFET device with the basic electrostatic parametric details, in figure 1.b equivalent capacitance of the GFET model, in figure 1.c view of the proposed model GFET with the equivalent capacitance of the GFET model of GFET.

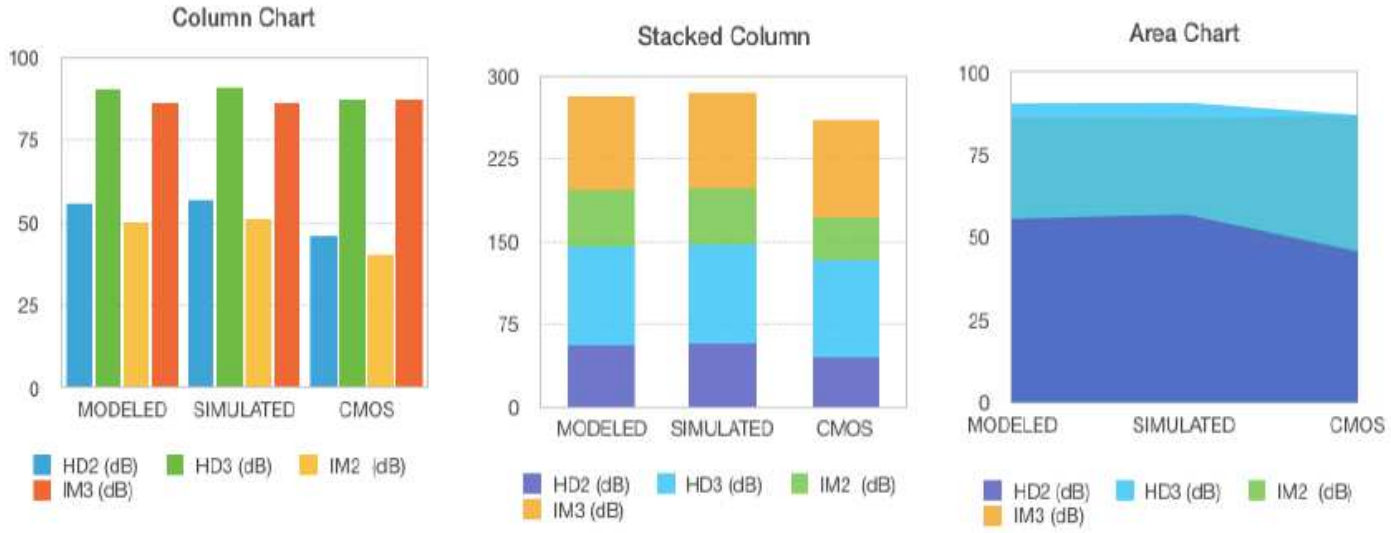

Figure 2

Non-linear behaviour of the bilayer graphene field effect transistors (GFET) shown with bar graph as the static nonlinearity by the column, stacked and area chart for the proposed modelled, and CMOS field effect devices.

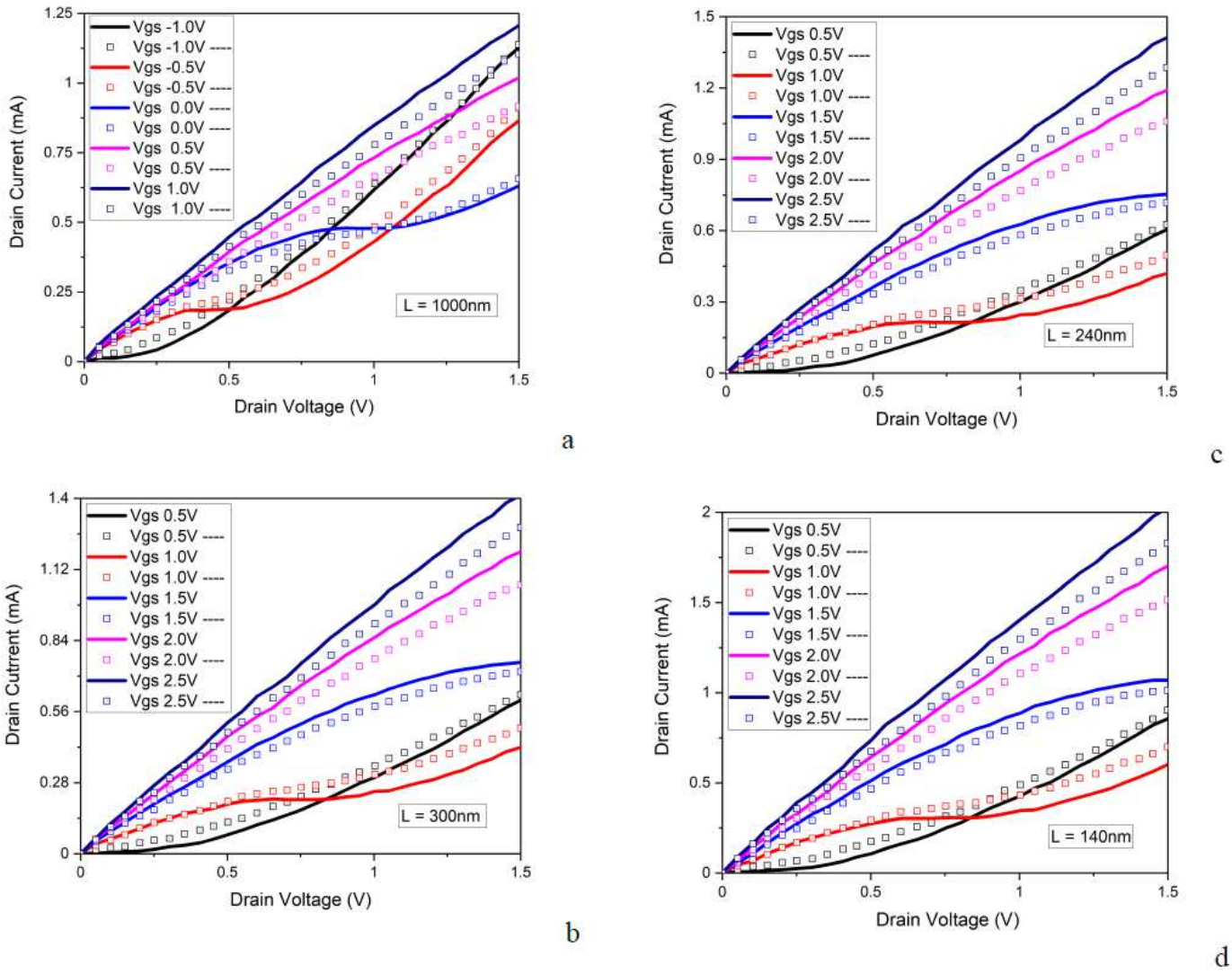

Figure 3

Non-linear characteristic behavior of the quasi-ballistic GFETs. figure 3.a Ids vs Vds output characteristic curve is showing highly nonlinear behavior of curve at 1000nm. Figure. 3.b at 300nm also shows nonlinearity at low (0 to 1V) drain voltage and shows linear shape after 1V drain voltage value. Figure 3.c shows the almost linear curve of current and voltage at 240nm, while a kink is present at 1.25V at a low gate voltage value. Figure 3.d is shown the linear curve of output drain current and voltage at all (0 to 2V) drain voltage at 140nm. All the simulated results are shown in figure 3 are drawn by lines while all the analytical outcome values are drawn by squares (symbols).